

Supporting Information

Cu-based metal-organic frameworks for highly sensitive X-ray detector

Zheng Li,^{ab} Shuquan Chang,^{*a} Haiqian Zhang,^a Yong Hu,^b Yulong Huang,^b Lu Au^b and Shenqiang Ren^{bcd}

^a College of Material Science and Technology, Nanjing University of Aeronautics and Astronautics, Nanjing, Jiangsu, 210016, China

^b Department of Mechanical and Aerospace Engineering, University at Buffalo, The State University of New York, Buffalo, New York, 14260, United States

^c Department of Chemistry, University at Buffalo, The State University of New York, Buffalo, New York, 14260, United States

^d Research and Education in Energy Environment & Water Institute, University at Buffalo, The State University of New York, Buffalo, New York, 14260, United States

E-mail: chsq@nuaa.edu.cn.

Table of Contents

The Synthesis of Cu-DABDT MOFs; Morphological and structural characterizations; Direct X-ray detection experiment; Attenuation efficiency calculation; Charge carrier mobility and lifetime product ($\mu\tau$) calculation; Sensitivity (S) of the X-ray detector.

Figure S1 (a) SEM photograph and EDS elemental mapping images of as-synthesized Cu-DABDT MOFs. (b) Energy dispersive X-ray spectroscopy spectrum of Cu-DABDT MOFs.

Figure S2 TGA of Cu-DABDT MOFs.

Figure S3 X-ray diffraction pattern of Cu-DABDT MOFs.

Figure S4 Magnetic properties of Cu-DABDT MOFs. (a) Magnetic field dependent magnetization under various temperatures. (b) Temperature dependence of magnetic susceptibility (χ) under 1000 Oe.

Figure S5 Electron paramagnetic resonance (EPR) spectra of DABDT and Cu-DABDT MOFs at 300K.

Figure S6 Calculated mass attenuation coefficients dependent X-ray photon energy for Cu-DABDT MOFs, reported SCU-12 MOFs and typical X-ray detection materials Cd(Zn)Te, α -Se and Si in the range of 1 - 200 keV. Notably, the attenuation coefficients of Cu-DABDT are close to those of reported SCU-12 in the range of 10-50 keV.

Figure S7 I-V curves for the Cu-DABDT X-ray detector measured under dark and X-ray radiation with various dose rates from -1 to 1 V.

Figure S8 Radiation robustness of Cu-DABDT detector under X-ray irradiation.

Table S1. The atomic and weight percentage of various elements in Cu-DABDT MOFs.

The Synthesis of Cu-DABDT MOFs.

All reagents were used as received. Cu-DABDT MOFs was prepared through the following method: 1 mmol 2,5-diamino-1,4-benzenedithiol dihydrochloride (DABDT) was added into 50 mL DMF in a 250 mL three-necked flask with stirring and nitrogen purging for 2 h. After DABDT is completely dissolved in DMF, 50 mL of $\text{CuCl}_2 \cdot 2\text{H}_2\text{O}$ (0.02 mM) aqueous solution was added by using a syringe pump (0.5 mL min^{-1}). Then, $\text{NH}_3 \cdot \text{H}_2\text{O}$ is used to regulate the pH of the system to 7 and stirring for another 6 h is necessary for completion of the reaction. Finally, the black precipitate was obtained by centrifugation with 6000 rpm for 15 min and alternately cleaned with deoxygenated DI water and acetone for three cycles to remove the unreacted raw materials, and the final products were dried at $70 \text{ }^\circ\text{C}$ under vacuum for 12 h.

Morphological and structural characterizations.

The morphological characteristics of Cu-DABDT were obtained by high-resolution transmission electron microscope (JEOL JEM 2010) and focused ion beam scanning electron microscope (Carl Zeiss AURIGA CrossBeam). X-ray diffraction (XRD) data was collected from 10 to 90° with a step of 0.02° on a Rigaku Ultima IV instrument. The Fourier transform infrared spectrum was collected from $1,000$ to $4,000 \text{ cm}^{-1}$ on a Bruker VERTEX 70 spectrometer. The thermalgravimetric analysis (TGA) was performed using a thermogravimetric analyzer (SDT Q600) with a constant rate of $10 \text{ }^\circ\text{C}/\text{min}$ from 50 to $1,000 \text{ }^\circ\text{C}$ under nitrogen flow. Renishaw inVia Raman microscope (Renishaw, Inc. Hoffman Estates, IL) was employed to acquire Raman data. Magnetic properties measurements were carried out using a Vibrating Sample Magnetometer (VSM, MicroSense EZ7-380V). The electron paramagnetic resonance (EPR) was measured on a Bruker ELEXYS E580 EPR spectrometer. The Kurt J. Lesker AXXIS Electron-Beam Evaporator deposited the Au

electrode. The temperature-dependent electrical conductivity of Cu-DABDT was conducted by the four-probe method on a Janis low temperature system with helium gas compressor (CTI-Cryogenics, Helix Technology Corp.) from 300 K to 50 K.

Direct X-ray detection experiment.

A Cu-DABDT-based radiation detector with symmetric structure Au/Cu-DABDT/Au was fabricated. The wafer of Cu-DABDT was pelleted by using mould with 6 mm diameter at 5 MPa. The 50 nm-thick gold electrode was deposited on two sides of wafer by electron-beam evaporator. The X-ray source is an Ag target MiniX X-ray tube (Amptek, Inc). X-ray tube voltage and current can be controlled from 10 to 50 kV and 10 to 200 μ A, respectively.

Attenuation efficiency calculation.

Attenuation efficiency (A) can be calculated as $A = 1 - e^{-\mu_L x}$, where x is the effective retarding thickness, μ_L is the linear attenuation coefficient, respectively. Here, the linear attenuation coefficient is defined as $\mu_L = \rho \mu_m$, where ρ is the density of materials and μ_m is the mass attenuation coefficient obtained from the photon cross sections database XCOM by NIST.

Charge carrier mobility and lifetime product ($\mu\tau$) calculation.

The $\mu\tau$ was obtained by modified Hecht equation: $I = \frac{I_0 \mu\tau V}{L^2} [1 - \exp(\frac{-L^2}{\mu\tau V})]$, where I_0 equal to saturated photocurrent, V corresponds to applied bias, and L is material thickness.

Sensitivity (S) of the X-ray detector

The sensitivity (S) of the X-ray device derived from $S = \partial J / \partial D$, where J and D is the current density and dose rate, respectively.

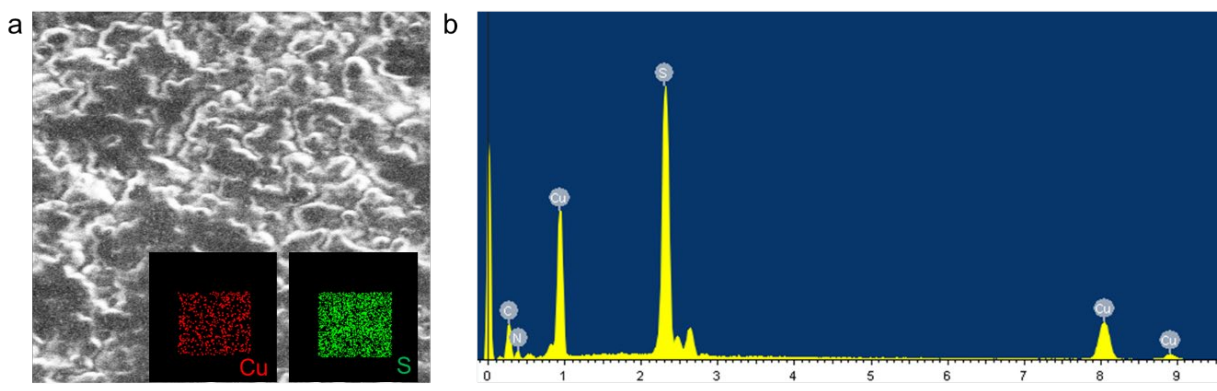


Figure S1 (a) SEM photograph and EDS elemental mapping images of as-synthesized Cu-DABDT MOFs. (b) Energy dispersive X-ray spectroscopy spectrum of Cu-DABDT MOFs.

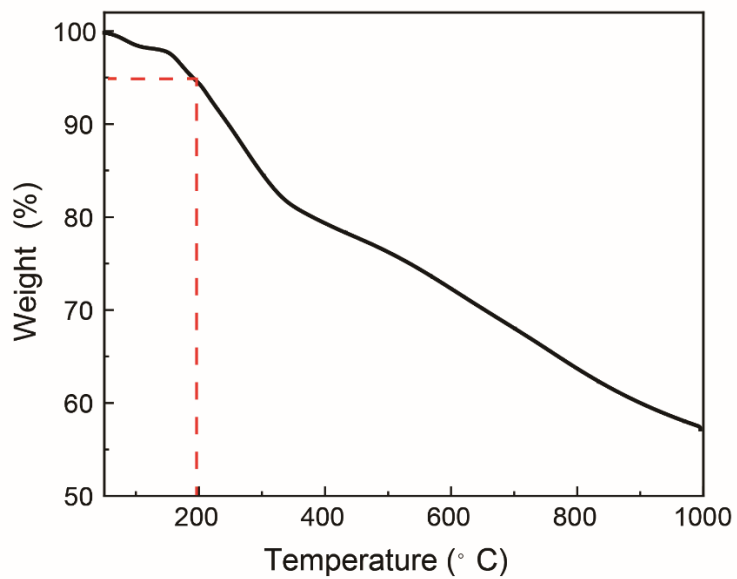


Figure S2 TGA of Cu-DABDT MOFs.

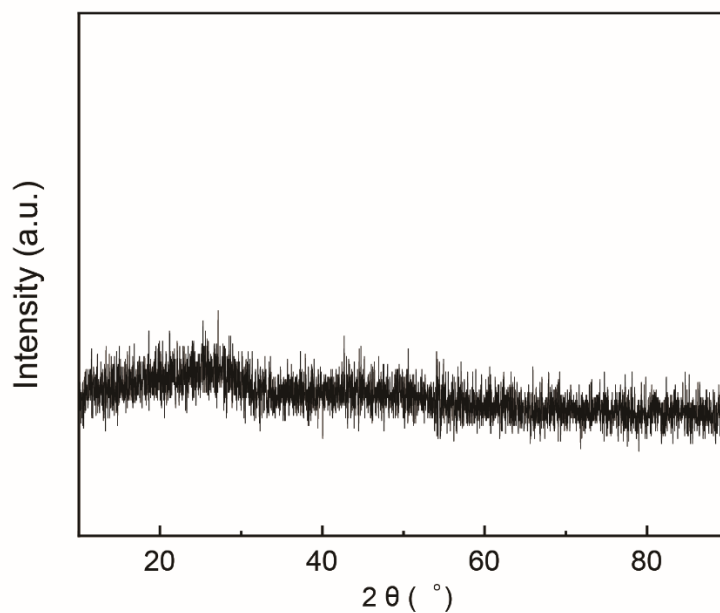


Figure S3 X-ray diffraction pattern of Cu-DABDT MOFs.

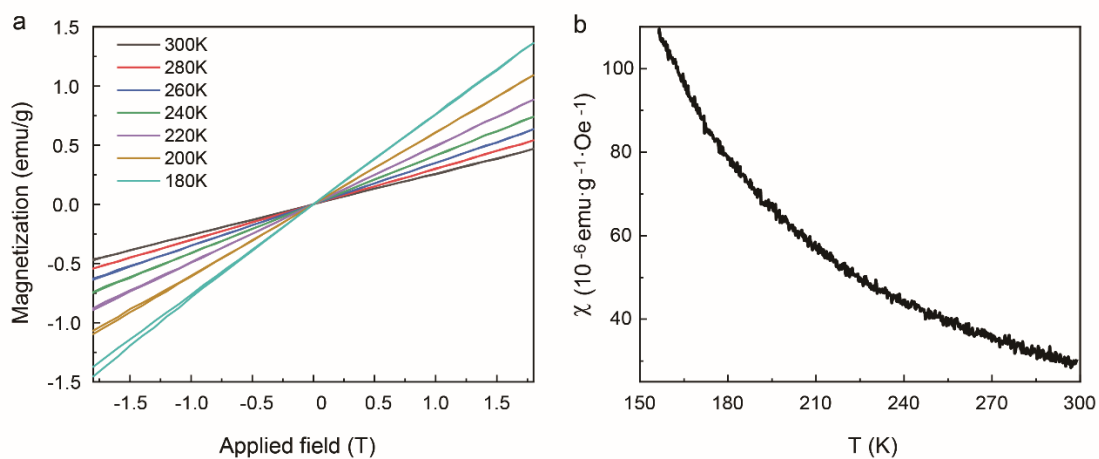


Figure S4 Magnetic properties of Cu-DABDT MOFs. (a) Magnetic field dependent magnetization under various temperatures. (b) Temperature dependence of magnetic susceptibility (χ) under 1000 Oe.

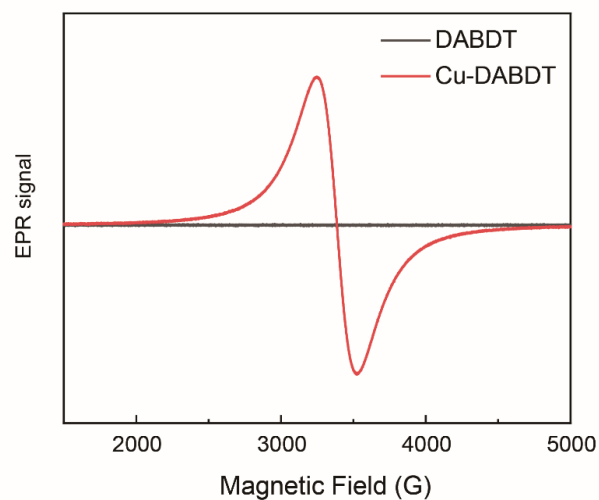


Figure S5 Electron paramagnetic resonance (EPR) spectra of DABDT and Cu–DABDT MOFs at 300K.

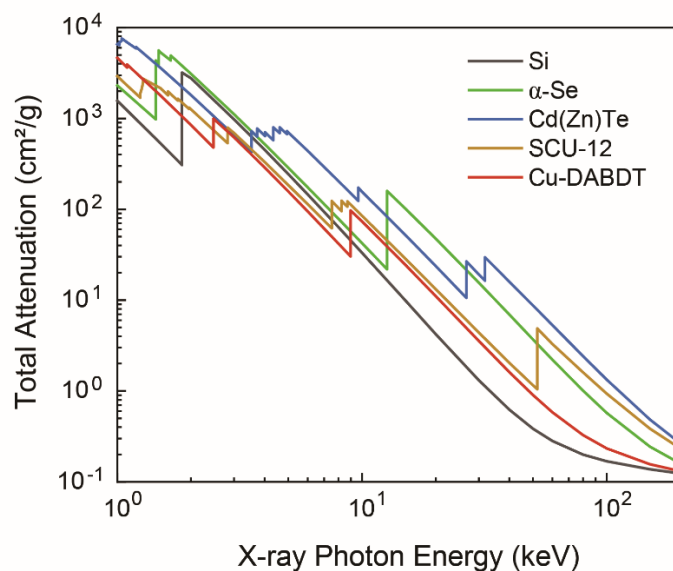


Figure S6 Calculated mass attenuation coefficients dependent X-ray photon energy for Cu-DABDT MOFs, reported SCU-12 MOFs and typical X-ray detection materials Cd(Zn)Te, α -Se and Si in the range of 1 - 200 keV. Notably, the attenuation coefficients of Cu-DABDT are close to those of reported SCU-12 in the range of 10-50 keV.

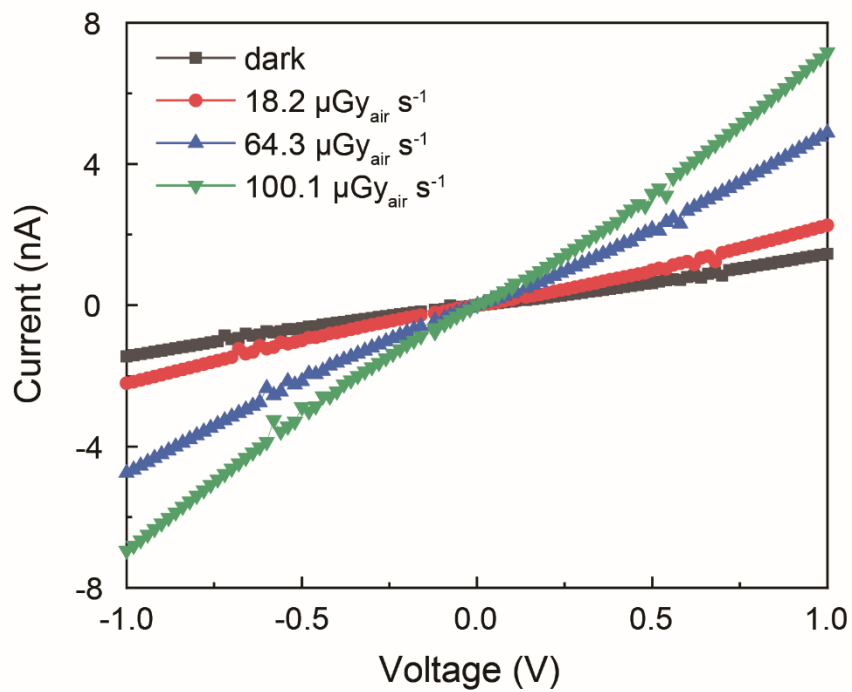


Figure S7 I-V curves for the Cu-DABDT X-ray detector measured under dark and X-ray radiation with various dose rates from -1 to 1 V.

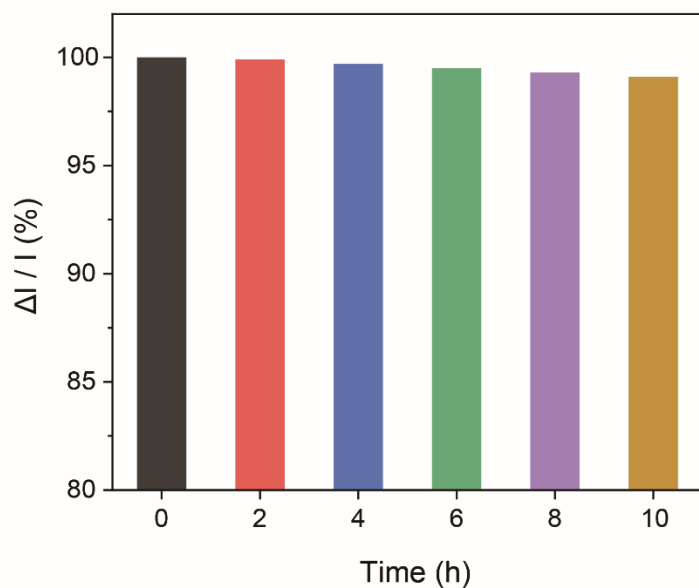


Figure S8 Radiation robustness of Cu-DABDT detector under X-ray irradiation.

Table S1. The atomic and weight percentage of various elements in Cu-DABDT MOFs.

Element	Weight%	Atomic%
C K	36.34	58.56
N K	14.48	20.00
S K	21.61	13.05
Cu L	27.57	8.40
Totals	100.00	